

Attosecond physics: facing the wave–particle duality

Markus Drescher^{1,2} and Ferenc Krausz^{3,4}

¹ Institut für Experimentalphysik, Universität Hamburg, Luruper Chaussee 149, 22761 Hamburg, Germany

² Fakultät für Physik, Universität Bielefeld, Universitätsstr. 25, 33615 Bielefeld, Germany

³ Max-Planck-Institut für Quantenoptik, Hans-Kopfermann-Strasse 1, D-85748 Garching, Germany

⁴ Department für Physik, Ludwig-Maximilians-Universität München, Am Coulombwall 1, D-85478 Garching, Germany

Received 17 December 2004

Published 25 April 2005

Online at stacks.iop.org/JPhysB/38/S727

Abstract

Recent progress in generation and control of intense optical fields has given rise to isolated soft x-ray pulses with durations significantly below 1 fs. These constitute a tool of unprecedented temporal definition for attosecond physics—the study and manipulation of electronic motion on a time scale approaching the atomic unit of time. A key mechanism in such experiments is the well-defined momentum transfer between a quasi-free electron, released from an atom following irradiation by a short x-ray pulse, and a precisely controlled strong visible light field. The electrons' final kinetic energy thus sensitively depends on the timing of electron release with respect to the field oscillations and reveals the ejected electrons' confinement in time with sub-cycle, i.e. attosecond, resolution. Experiments resulting in electron emission of different durations can be interpreted in terms of a particle-like or wave-like electron, depending on whether the emission duration is considerably shorter or longer than the wave period of the probing light.

1. Introduction

The interpretation [1] of disturbing experimental findings [2] in the photoeffect in conjunction with the subsequent fundamental work in quantum physics at the turn of the 20th century forced us to accept the dual nature of light and matter as having both particle and wave properties. As confirmed in many experiments, matter reveals a particle or wave character depending on the question asked, i.e. the type of experiment conducted. In this paper, we discuss how observation of the interplay between light and matter *in the time domain* allows one—in the same experiment—to interrogate the particle and the wave nature of an electron simultaneously. The length of the temporal interval over which electrons are set free to interact with the light field (in the terminology of quantum mechanics: the duration of the electron wave packet) in relation to the oscillation period of the light wave decides which property

dominates. By varying the temporal width of the probing light ‘gate’ or the duration of the particle wave packet, the transition between classical and quantum-mechanical behaviour can be studied.

A comprehensive formal consideration of both wave properties (e.g. oscillation and interference) and particle properties (e.g. momentum and spatial confinement) is provided by the wave packet concept [3] as a suitable superposition of extended waves within a certain frequency interval. Via Fourier transform, the interval of contributing wave frequencies determines the temporal and longitudinal spatial extents of the wave packet. Well-defined freely propagating light wave packets can be obtained from modern pulsed laser systems [4] with a time-bandwidth product close to its minimum possible value (Fourier-limited pulse). The photoeffect serves as a mediator for converting a light wave packet into a matter (= electron) wave packet in a highly coherent fashion. In our approach, an electron wave packet is launched from atoms ionized by an XUV pulse to interact with the strong field of a pulse of visible laser light. The relative time scales of the electron wave packet and the probing light field appear to determine the observed character of the electron.

If the electron wave packet’s duration τ_e is considerably shorter than the light oscillation period T_L , $\tau_e \ll T_L$, particle-like behaviour is observed; if $\tau_e \gg T_L$, the wave nature will dominate. From an experimental point of view, the latter condition is much easier to meet because it relies on rather long—fs to ps—ionizing pulses which can be delivered from a number of sources [5]. Observation of particle-like behaviour, however, is much more demanding; probing with a light field of period $T_L \approx 2.5$ fs (red light) calls for XUV pulses with a duration $\tau_x < 1$ fs. It is only the recent progress in generation of attosecond ($1 \text{ as} = 10^{-18} \text{ s}$) XUV pulses that allows us to unveil the particle character of electrons in such experiments and study the gradual transition in their behaviour to propagation in the form of waves.

In section 2, we introduce the photonic tools necessary for our technique: (i) phase-controlled few-cycle intense laser pulses and (ii) isolated sub-femtosecond XUV pulses. In the following sections, the electron’s particle or wave character will manifest itself in experimental examples for the cases $\tau_e \ll T_L$ and $\tau_e \gg T_L$, respectively. The former case provides an illustrative picture for introducing the basic concept of probing the electron emission with a rapidly varying electromagnetic field. The interaction of sub-femtosecond electron emission with a fully controlled (few-cycle) optical wave permits the time-domain characterization of sub-fs XUV pulses as well as of the electric field of visible light in a classical framework, constituting the first manifestations of attosecond metrology. The same type of experiment reveals the wave-like nature of the electron if its emission lasts longer than T_L . In our experiments, an electron wave packet with this property results from secondary electron emission due to atomic Auger decay following ionization. A suitable choice of experimental parameters allows one to generate situations where $\tau_e \sim T_L$. For such intermediate cases, the electron exhibits particle and wave properties simultaneously.

2. Basic concepts and tools of attosecond metrology

Access to ultrafast phenomena relies on the measurement of brief time intervals, which, in turn, requires a physical quantity that varies fast in a controlled and reproducible manner. In femtosecond metrology, the amplitude envelope $E_a(t)$ of the electric field

$$E_L(t) = E_a(t) \cos(\omega_L t + \varphi) \quad (1)$$

of a femtosecond laser pulse (of carrier frequency ω_L) takes over the role of this quantity. In the shortest pulses, the rise time of the field amplitude is as brief as a few femtoseconds [6] and

permits metrology with a resolution approaching 1 fs. Pump–probe techniques furnished with this time resolution opened the way to observing for the first time the breakage and creation of chemical bonds by tracing the motion of atoms within molecules in real time [7]. Extension of this capability to electronic motion deep in the interior of atoms and molecules requires new tools, because the characteristic time scale for this class of microscopic dynamics is defined by the classical Bohr orbit time of the electron in the ground state of hydrogen, which amounts to some 150 as.

Metrology on this time scale requires controlled variation of a physical quantity within 1 fs. Given the fact that the field oscillation period of visible light is longer than 1 fs, this definitely cannot be achieved with $E_a(t)$. However, the hyperfast variation of the oscillating electric field of the laser pulse does meet the speed criterion for attosecond metrology. In fact, the electric field of 750 nm radiation (emitted by titanium:sapphire-laser-based femtosecond systems) changes from zero to its maximum within some 625 as, providing a sufficiently rapid slope for attosecond measurements.

In principle, time-domain measurements referenced to the laser electric field do not strictly rely on a short duration of the laser pulse. Triggering the microscopic motion to be studied and performing the attosecond measurement repeatedly cycle-by-cycle by exploiting correlation [8] may obviate the need for a very short laser pulse. Because the measurement is accumulated over several or many laser cycles in this case, it has to be ensured that (i) the sub-laser-cycle dynamics evolves the same way and (ii) is referenced to the same clock from cycle-to-cycle during the measurement period. In general, it is hard to meet these requirements with high precision, which means that the implementation of this concept to a wide range of problems is not straightforward.

The above difficulties can be avoided in a natural manner by triggering the sub-cycle dynamics only once per laser pulse. This requires a cycle that can be distinguished from all the others in the pulse. Isolation of a single cycle is straightforward in a pulse comprising merely a few oscillation cycles. Intense few-cycle pulses can now be routinely produced [9]. The amplitude of the central wave cycle in such a pulse is significantly higher than that of any other cycles, allowing discrimination. The central wave cycle of a few-cycle pulse therefore lends itself to *both* getting an attosecond process going *and* providing the reference clock for measuring it. Both of these operations call for well-controlled, well-reproducible field evolution.

Reproducible field evolution from one laser pulse to the next requires that the timing of the oscillations with respect to the pulse peak can be reproduced. In the carrier–envelope representation of the light field as given by (1), this timing is mathematically denoted by φ , which has been referred to as the carrier–envelope phase. $\varphi = 0$ in the representation of (1) implies a waveform that has one single most intense half oscillation cycle at the centre of the pulse. We call this a *cosine waveform*. $\varphi = -\pi/2$, on the other hand, results in a waveform with two equally strong half cycles. In our terminology, this is a *sine waveform*. These waveforms (figure 1) constitute two specific examples out of an infinite number of possibilities for the same amplitude envelope $E_a(t)$ and carrier frequency ω_L . Few-cycle pulses with a controlled waveform, i.e. controlled value of φ , open the way to attosecond control and metrology in a natural way.

Unfortunately, conventional ultrashort-pulse lasers do not deliver pulses with a constant waveform. Rather, the carrier–envelope phase is subject to a pulse-to-pulse shift as a consequence of the difference between the group and phase delays in the laser cavity. This pulse-to-pulse phase shift had been measured as early as 1996 [10], but stabilization of the shift [11–13] became possible only years later, drawing on a proposal by Hänsch [14–16]. These carrier–envelope-phase-stabilized femtosecond oscillators [11, 13] revolutionized frequency

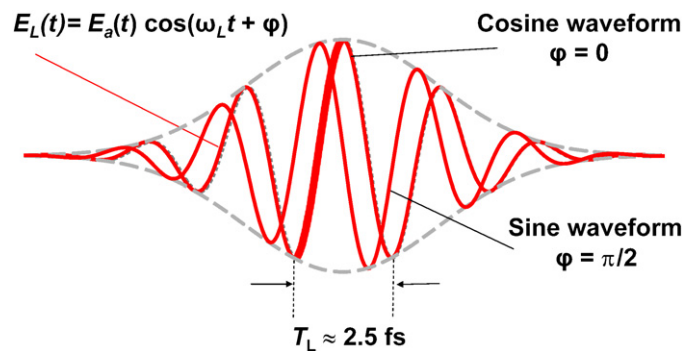


Figure 1. Few-cycle light waves of identical amplitude envelope and carrier frequency carried at a wavelength of 750 nm. Different values of the carrier-envelope phase result in different, in our example cosine- and sine-shaped, waveforms. If the waveform is reproducible (from laser pulse to laser pulse), the rapidly varying field within, for example, the half cycle highlighted can be used as a reference clock for time-domain measurements on a sub-femtosecond time scale.

metrology owing to their precisely controlled frequency comb, but had virtually no impact in the time domain because the sensitivity of light-matter interactions to the waveform relies on field strengths higher than that available from oscillators. Collaboration between one of the authors' groups with that of Hänsch recently led to the generation of waveform-reproducible intense few-cycle pulses [17].

The first source of phase-stabilized high-power few-cycle laser pulses delivers 5 fs, 0.1 TW pulses at a wavelength of 750 nm and a repetition rate of 1 kHz (figure 2). Whilst the control loops in figure 2 permit stabilization of φ as well as changing it by a known amount, the absolute value of φ is still unknown and remains to be determined from strong-field experiments. These waveform-controlled few-cycle pulses have opened the door to control the motion of electrons in and around atoms within the wave cycle, i.e. on a sub-femtosecond time scale. Sub-wave-cycle electron dynamics naturally unfold in the process of optical field ionization. This phenomenon is predicted to set in at laser field strengths yielding a cycle-averaged wiggling energy of a free electron (ponderomotive potential) comparable to or larger than the binding energy of valence electrons, which is typically fulfilled at intensity levels beyond $10^{14} \text{ W cm}^{-2}$ in the near-infrared spectral range.

A linearly polarized intense light wave detaches electrons from the irradiated atoms whenever the electric field exceeds the threshold for tunnel ionization (near the oscillation peaks). The liberated electrons are first removed from the atomic core, but the laser field changes its direction and pulls the electrons back to their original location less than a period later, resulting in a recollision of the electron wave packets with their parent ions. This recollision gives rise, with some probability, to recombination of the electron into its original bound state and to simultaneous emission of an energetic (extreme ultraviolet or soft-x-ray) photon. The phenomenon has been modelled by Lewenstein *et al* [18] on the basis of the above-outlined intuitive picture put forward by Corkum [19] and independently by Schafer *et al* [20]. If the driving laser pulse consists of many wave cycles, this process is repeated quasi-periodically each half cycle. Hence, theory predicts the light emission in the form of a quasi-periodic train of sub-fs bursts with a spectrum consisting of high-order harmonics of the incident laser field. This time structure was recently confirmed experimentally [21, 22].

In the case of a few-cycle driver, only a few recollisions occur. The electron wave packet recolliding near the zero transition of the laser field following the pulse peak is

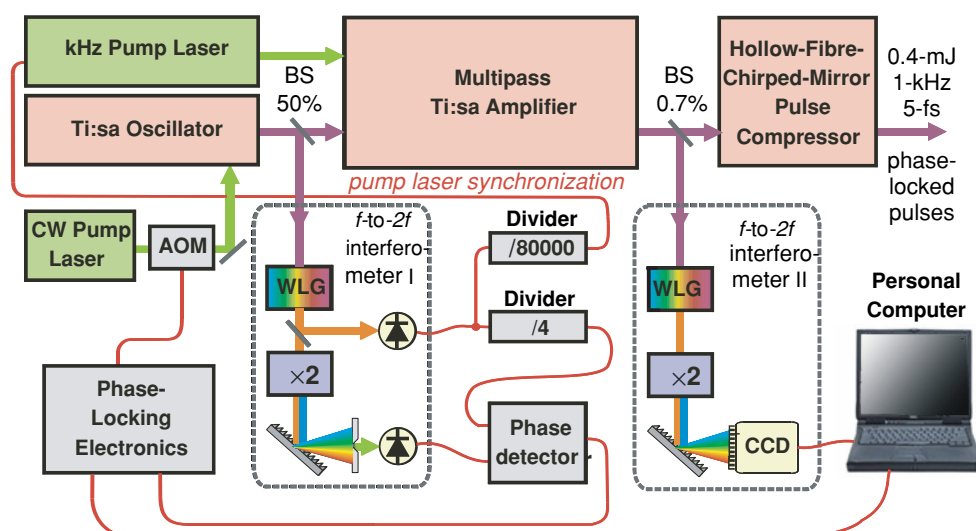


Figure 2. Overview of a carrier–envelope–phase–stabilized, i.e. waveform–controlled, few–cycle laser source. The phase of the pulses emitted from the Ti:sapphire oscillator is maintained by a frequency–domain (f -to- $2f$) technique originally developed for frequency–domain metrology, through a feedback loop controlling the pump power with an acousto–optical modulator (AOM). The energy of the phase–stabilized pulses is boosted by approximately six orders of magnitude in a multipass amplifier (Femtopower Compact Pro, Femtolasers GmbH) and compressed to a duration of 5 fs in a gas–filled–hollow–fibre/chirped–mirror compressor. Random phase drifts in the amplifier are monitored with Interferometer II and pre–compensated in the oscillator to yield waveform–controlled few–cycle pulses with excellent long–term stability.

significantly more energetic than the others, because it is pulled back by the most intense half cycle to the vicinity of the core. This implies the emergence of a burst at higher photon energies than other recollision events. For a cosine waveform, we expect one single highest energy XUV burst to be emitted (figure 3(a)), whereas a sine waveform—comprising two half cycles of highest amplitude—will create a couple of pulses at the highest photon energies (figure 3(b)).

These considerations suggest that waveform–controlled few–cycle light can excite electronic motion in a controlled manner within the oscillation cycle of visible light, i.e. on a sub–femtosecond time scale. The resultant sub–femtosecond extreme ultraviolet emission, in turn, can be used to test the ability of controlled light field oscillations to perform measurements on an attosecond time scale. To this end, the XUV radiation together with the few–cycle laser pulse used for generating it are focused into a second atomic gas jet (figure 4). The laser field is strong enough to change significantly the momentum of the electrons knocked off by XUV photons. The momentum change—measured by time–of–flight spectrometry—is directed parallel to the electric field vector and depends on the instant of release of the electron wave packet within the laser cycle.

The sensitive dependence of the momentum change of the freed electrons on the phase of the field at the instant of their release *and* precise control over the hyperfast light field oscillations permit probing of the ejected wave packet with sub–femtosecond resolution. Depending on the emission duration of the electron wave packet as compared with the wave period of the probing laser light, the electron reveals particle–like or wave–like behaviour in its interaction with the light field, as is discussed in the following sections.

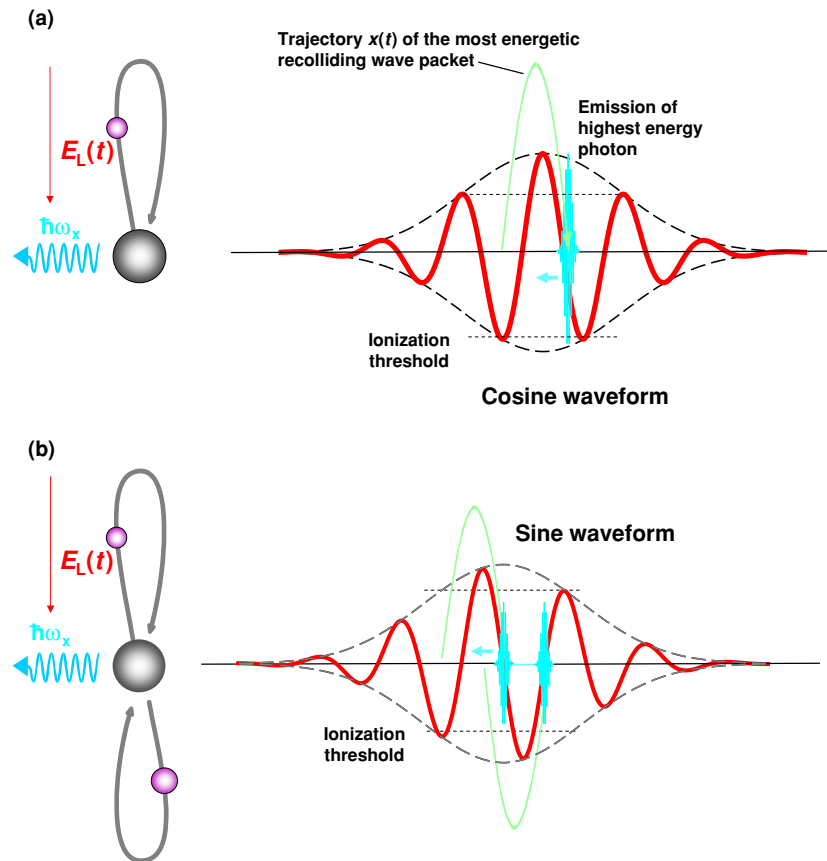


Figure 3. Schematic illustration of XUV emission from atoms ionized by a linearly polarized few-cycle laser pulse. The most-weakly bound atomic electron is detached with some probability from the atom as the laser electric field exceeds the optical-field-ionization threshold (black dashed line). The electron wave packet is first removed and then pushed back to the vicinity of the core. The most energetic part of the electron wave packet recollides at the zero transition of the driving electric field, resulting in emission of the most energetic photons in one or two bursts of sub-femtosecond duration for (a) a cosine- and (b) a sine-shaped driver wave, respectively.

3. Particle-like behaviour: sub-femtosecond pulse characterization

Let us consider photoionization of an atom in the presence of a visible laser field too weak to induce directly or even to influence the electron emission process. As the ionization can be assumed to occur instantaneously on the time scale under consideration, excitation with an ultrashort XUV pulse of duration $\tau_x \ll T_L$ forms an electron wave packet with an envelope mimicking the photon wave packet, $\tau_e \sim \tau_x$. Owing to this temporal confinement, we could consider this escaping photoelectron as a particle with a defined initial momentum p_i . Once liberated, however, the electron experiences the laser field and is accelerated in the direction of the light polarization, thus gaining or losing momentum, $\Delta p = p_f - p_i$. In momentum space, this transfer can be regarded as an alternating linear displacement of the momentum sphere [23] as depicted in figure 5, where isotropic electron emission is assumed. From this classical scheme, it becomes clear that the momentum transfer Δp depends on the angle between p_i and the laser polarization plane, but most importantly on the phase and amplitude of the laser field

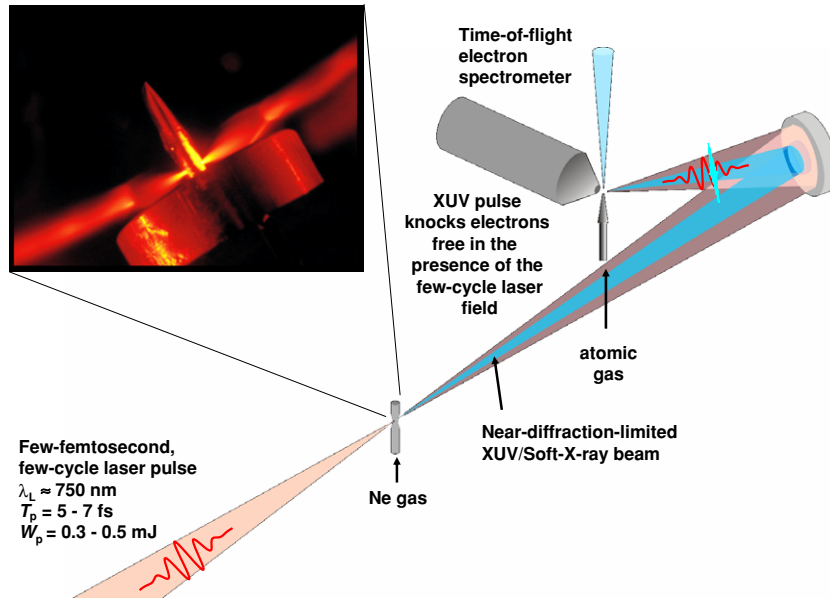


Figure 4. Schematic of the experimental set-up for generation of sub-femtosecond XUV pulses and their use for impulsive atomic excitation in the presence of a waveform-controlled few-cycle light wave. The extreme ultraviolet radiation emerging from a tube filled with neon gas as a result of the interaction depicted in figure 3 is emitted in a highly collimated laser-like beam propagating collinearly with the generating laser beam in an evacuated beamline. The two beams are reflected by two different parts of a composite molybdenum–silicon multilayer mirror. The two concentric parts can be translated with respect to each other, allowing one beam to be delayed with attosecond precision with respect to the other. Both beams are focused into a second atomic gas target which is excited by the XUV pulses in the presence of the laser field. The freed electrons are detected and analysed with a time-of-flight spectrometer.

at the instance of electron injection, i.e. the ionization event. Δp is parallel with the electric field vector in a linearly polarized light field with its magnitude given by

$$\Delta p = e \int_t^\infty E_L(t') dt' = eA_L(t), \quad (2)$$

where $A_L(t)$ is the vector potential. Δp vanishes when the ionization takes place in the field maximum and is strongest for the zero field transitions a quarter of a light period earlier or later. This corresponds to a 90° phase shift between the light oscillation and the observed momentum transfer, independent of the exact form of the pulse envelope $E_a(t)$.

The validity of this classical picture of particle-like electrons interacting with a synchronized light field is put to the test in an experiment depicted in figure 6, utilizing sub-fs XUV pulses well synchronized with a phase-stabilized few-cycle laser field as introduced in the previous section. Free atoms are ionized with the (pump) XUV pulse and the escaping photoelectrons are probed with a delayed light field. Varying the delay Δt between the XUV and laser pulses, one should expect an alternating bipolar shift of the final kinetic electron energy W_f measured in the spectrometer according to

$$W_f(\Delta t) = W_i + \sqrt{8W_i k E_a^2(\Delta t) \sin(\omega_L \Delta t)}, \quad (3)$$

with $k = e^2/4m_e\omega_L^2$.

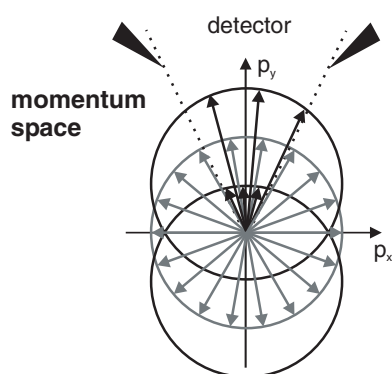


Figure 5. Schematic picture of the momentum transfer imposed on a photoemitted electron by a strong light field, polarized vertically in this figure. An initially isotropic distribution (grey) of photoelectrons with equal momentum (length of arrows) is modulated by the addition of a constant momentum equivalent to the vector potential of the light field at the instant of electron emission. Accordingly, the momentum transfer directly follows the oscillation of the vector potential. The most pronounced variation is observed in the light polarization direction.

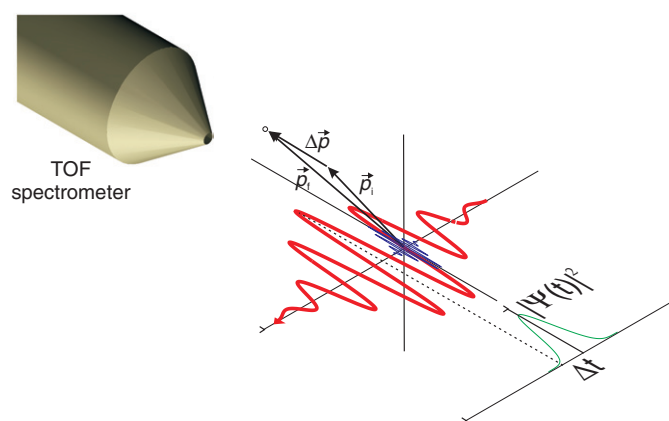


Figure 6. Observation of electron wave packets shorter than the light oscillation cycle. XUV and laser pulses travel collinearly and with fixed relative delay through an atomic gas. The photoeffect transforms the XUV photon wave packet into an electron wave packet of the same temporal shape. Upon emission, the electron immediately experiences the laser field and gains or loses kinetic energy, depending on the temporal delay. This kinetic energy shift is most pronounced in the direction of the laser field polarization, where a time-of-flight electron spectrometer is situated.

Figure 7 presents the result for a corresponding experiment on neon atoms excited with an 8 eV wide XUV pulse centred at a photon energy of 92 eV [24]. The particle-like behaviour is clearly evident in the oscillatory pattern of the Ne 2p photoelectrons. The extreme sensitivity of the electron energy on the light phase provides the footing for temporal measurements with a resolution of a fraction of the laser period. Analysis of figure 7 results in a XUV pulse duration of $250 + 30/-5$ as and proves that our XUV source delivers isolated pulses rather than pulse trains. The shortness of these pulses has provided a δ -like gate for a first-time sampling of the temporal evolution of a visible light field [25].

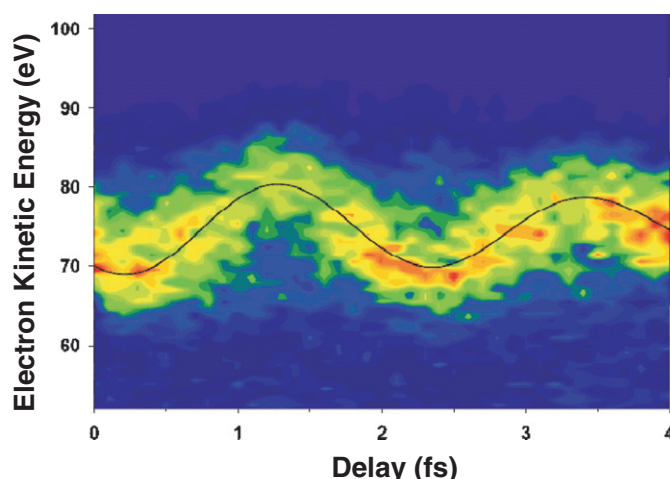


Figure 7. Experimental result from a measurement as depicted in figure 6. Excitation of neon atoms in an 8 eV wide band centred around a photon energy of 93 eV yields Ne-2p photoelectrons at a kinetic energy of approximately 72 ± 4 eV. Momentum transfer between the photoelectron and the laser field leads to the observed oscillatory energy shift directly mapping the vector potential of the light field. This is a signature for particle-like behaviour of the electron. Analysis of this distribution results in a duration of $250 +30/-5$ as for the electron wave packet, i.e. the XUV pulse, and so the condition $\tau_e < T_L$ is safely met.

4. Wave-like behaviour: sampling secondary electrons

Relaxation processes in atoms give rise to delayed electron emission in the form of electron wave packets with a shape and temporal extension characteristic of a specific decay (figure 8). Sampling the temporal profile of such wave packets thus reveals details of the underlying electronic dynamics with attosecond precision. For many atomic shells, the typical decay time is of the order of several femtoseconds, thus extending over a few laser field cycles. For such cases, the outgoing electron wave packet will interact with the light field at a multitude of different relative phases as depicted in figure 9. Coherent superposition of all contributions leads to the formation of sidebands [26] in the electron kinetic energy spectra—a signature for wave-like behaviour.

One of the most comprehensively studied (in the energy domain) systems of atomic relaxation is nonresonant MNN Auger decay in krypton following excitation of the 3d shell above the ionization threshold at 93.8 eV [27]. Time-resolved measurement of the characteristic exponential decay time τ_h of the core-hole decay relies on sampling of the Auger electron wave packet formed after excitation of krypton atoms with an XUV pulse in a 3 eV wide band centred at 97 eV, corresponding to a (Fourier-limited) duration of 0.9 fs. A typical electron spectrum acquired in the time-of-flight spectrometer is shown in the upper right corner of figure 10. Combining such spectra taken at different delays Δt between the XUV and the laser pulse provides a map of the temporal evolution of the electron emission, displayed as a surface plot in figure 10. According to the above discussion for electron emission with $\tau_e \gg T_L$, interaction with the laser field leads to the emergence of sidebands separated by multiples of $h\nu_L \sim 1.6$ eV from each Auger line. For the case of the $M_{4,5}N_1N_{2,3}$ Auger lines investigated here, this spacing approximately coincides with the typical separation between the Auger lines [28], thereby obscuring most of the sidebands. Only for the least energetic (1P_1) line is the first sideband well isolated and taken into consideration. Since the

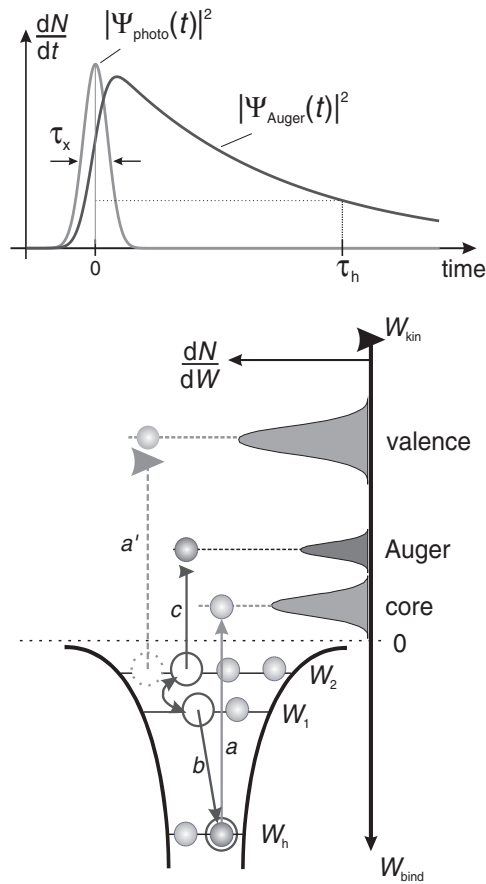


Figure 8. Lower panel: scheme of the Auger decay. Sufficiently high photon energies can create an inner-shell hole upon emission of a photoelectron (a). The vacancy is spontaneously filled with a less bound electron (b). The binding energy of the latter is transferred to a third (Auger) electron leaving the ion with defined kinetic energy (c). Upper panel: since the Auger decay is a spontaneous relaxation process, the secondary Auger wave packet $\Psi_{\text{Auger}}(t)$ should follow an exponential decay law. It will therefore, in general, be more extended in time than the primary photoelectron wave packet $\Psi_{\text{Photo}}(t)$.

sideband area represents a convolution of the Auger emission rate and the laser pulse envelope $E_a(t)$, the latter must be precisely known to extract the desired value of τ_h . In accordance with the technique for light field mapping introduced in the previous section, this calibrating information is simultaneously embedded in the acquired electron spectra of the 4p photo line. With this information as input, a fit procedure with τ_h as the only varied parameter is capable of extracting the temporal evolution of the Auger emission rate. This analysis yields $\tau_h = 7.9(+1.0/-0.9)$ fs for the lifetime of $M(3d_{5/2})$ vacancies in krypton [29]. Assuming monoexponential decay, this lifetime corresponds to a natural linewidth of $\Gamma = \hbar/\tau_h = 84 \pm 10$ meV, well in accordance with the energy-domain result of 88 ± 4 meV from [30].

As evident from figure 10, a wave-like character is clearly perceptible already for $\tau_e \sim 3T_L$. Typical time constants of atomic decay processes, however, cover a range from 0.1 fs to 10 fs [31]. In many cases, one therefore faces situations where $\tau_e \sim T_L$ suggests behaviour intermediate between the particle and wave limits. In a quantum mechanical calculation, the

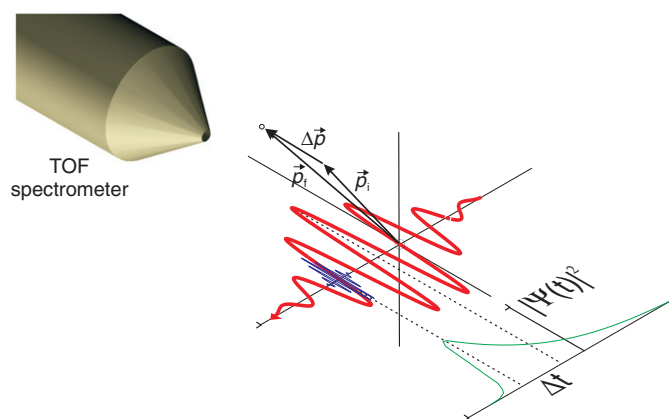


Figure 9. Experimental arrangement for observation of electron wave packets longer than the light oscillation cycle. XUV and laser pulses travel collinearly and with fixed relative delay through an atomic gas. In contrast to the experiment depicted in figure 6, the electron wave packet is longer than the exciting XUV pulse due to an intrinsic atomic process, e.g. Auger decay. Different parts of the wave packet experience different phases of the laser field; the resulting coherent superposition leads to an interference pattern in the electron spectra.

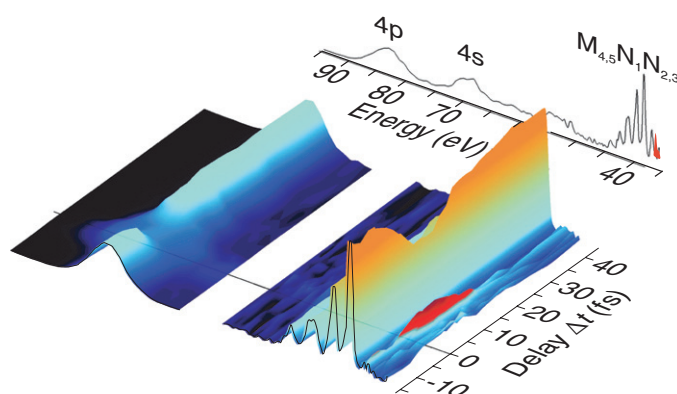


Figure 10. Experimental result from measurement of the time evolution of MNN Auger decay in Kr using the set-up depicted in figure 9. The delay-dependent plot is composed of spectra as shown in the upper right corner. The temporally extended coherent interaction between Auger electrons and the laser field leads to the transient formation of spectral sidebands of the Auger lines (red), from which the inner-shell relaxation dynamics can be retrieved. To this end, simultaneously acquired broadening of the 4p photoelectron line provides important information about the temporal shape of the laser field envelope.

steady transition of time-resolved spectra from the particle to the wave case has been followed [29, 32]. Figure 11 presents quantum mechanical simulations of Scrinzi and Yakovlev [29] of electron spectra assuming different lifetimes of a model Auger decay with a field-free kinetic energy of 40 eV. At $\tau_e = 5$ fs ($\tau_e = 2T_L$) the sideband pattern discussed above clearly dominates. For $\tau_e = 200$ as ($\tau_e = T_L/12.5$), on the other hand, the well-expressed oscillation closely resembling the photoelectron study in figure 7 reveals the particle character of secondary electrons emitted almost instantaneously after excitation. Already for $\tau_e = 500$ as ($\tau_e = T_L/5$), contributions from the coherent interaction with different visible field phases

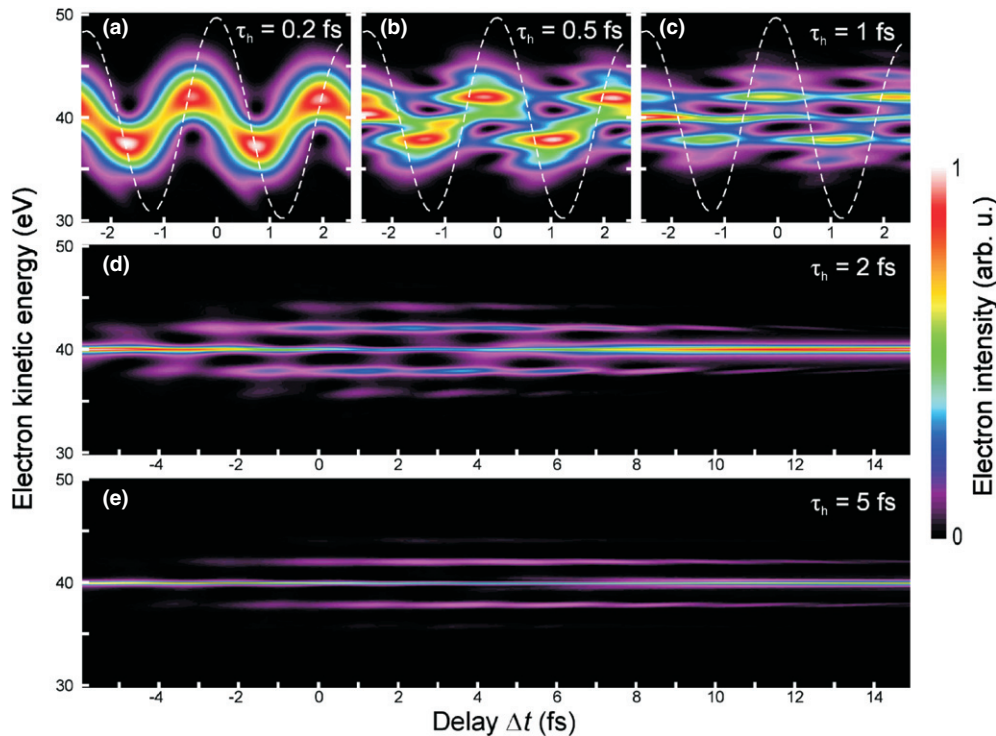


Figure 11. Simulation of time-resolved electron spectra for hypothetical Auger decay at various time constants for the atomic relaxation. An initial kinetic energy centred around 40 eV is assumed. The figure visualizes the gradual transition from a particle-like character of the electrons for very short electron wave packets, revealed by an oscillatory dependence of the spectra on the temporal delay, to a clear signature of wave-like behaviour in the form of spectral sidebands.

become clearly visible. A complex pattern in the range of $T_L/5 < \tau_e < T_L$ fully reveals the dual nature of matter with contributions from the particle (oscillation) and the wave (sidebands) behaviour becoming simultaneously observable.

5. Conclusion

Electric and/or magnetic fields are often used to affect the motion of electrons and probe their characteristics. Attosecond metrology now allows one to uncover wave- or particle-like behaviour of electrons emanating from the photoeffect induced by ultrashort XUV excitation. If the emission time of the electron is long in relation to the wave cycle of probing light ($\tau_e \gg T_L$), sidebands spaced by the laser photon energy from the main line appear in the energy spectrum of electrons emitted in the presence of a strong light field. This phenomenon results from interference between electron wave packets released at instants differing by the laser period (or its integer multiple) and is a clear manifestation of the wave nature of electrons. *The electrons behave like a coherent collective matter wave.* In the limit of $\tau_e \ll T_L$, this temporal interference is completely suppressed and the electrons' motion can be modelled and their momentum and energy can be precisely predicted in the framework of classical physics. *The electrons behave like a shower of particles with a point-like charge.* These two limits can, in principle, also be realized by varying the frequency of the light wave used for probing the electrons released by the photoeffect or Auger effect. It may thus be concluded

that, depending on the oscillation period of the probing field relative to the emission time, the electrons behave as a coherent matter wave or as point-like particles in their interaction with the electromagnetic field.

From a practical point of view, the intermediate regime $\tau_e < T_L$ or $\tau_e \sim T_L$ appears to be most important for the emerging field of attosecond science. In this regime, the electrons' energy and momentum distributions are modified gently and in a well-defined manner by the rapidly varying field. From the modified momentum and/or energy distributions, it is possible to determine the temporal structure of the electron emission. Probing the emission of primary (photo) and secondary (Auger) electrons created by impulsive (attosecond) excitation in this way yields direct time-domain information of the evolution of the underlying atomic excitation and relaxation processes, respectively.

The resolution of optical-field sampling of electron emission is dictated by the initial kinetic energy W_i of the ejected atomic electrons, by T_L and (as always) by the signal-to-noise (S/N) ratio. The briefest time interval within which two different atomic events can be recognized as different by this technique is ultimately limited by quantum-mechanical uncertainty, which dictates that any short time structure comes with a broad energy spectrum. To be able to resolve the spectral 'images' of two events separated in time by δt , they must be shifted with respect to each other in the final energy spectrum of the electrons by as much as at least their own spectral width $\delta W \approx \hbar/\delta t$. This requirement makes the resolving power

$$\delta t = \frac{T_L}{2\pi} \sqrt{\frac{\hbar\omega_L}{\Delta W_{\max}}}, \quad (4)$$

where ΔW_{\max} stands for the energy shift suffered by the electron ejected at the peak of $A_L(t)$. In recent measurements ΔW_{\max} approached 30 eV, yielding (for $T_L = 2.5$ fs) $\delta t \approx 100$ as [24]. Attosecond metrology based on interaction of electrons with a strongly controlled wave of intense few-cycle light is able to distinguish two ultrafast atomic events following each other within 100 as, constituting the shortest interval of time directly measurable to date.

Recent experimental advances afford promise of generation of single attosecond bursts with durations well below 100 as and photon energies approaching 1 keV [33]. At these excitation energies ΔW_{\max} can be enhanced by at least an order of magnitude, yielding $\delta t \approx 30$ as. Extension of the presented experiments to exploring simultaneously the sub-femtosecond temporal variation of emission intensity and momentum distribution of primary (photo) and secondary (Auger) electron emission will provide unprecedented insight into the complex excitation and relaxation dynamics of the electronic shell of atoms and molecules with a resolution that will approach the atomic unit of time (24 as).

Acknowledgments

For their invaluable contributions to the reported work, we thank A Baltuska, F Bammer, P Corkum, E Goulielmakis, U Heinzmann, M Hentschel, R Kienberger, U Kleineberg, N Milosevic, G A Reider, M Uiberacker, A Scrinzi, C Spielmann, G Tempea, V Yakovlev and Th Westerwalbesloh. The research has been sponsored by the FWF (Austria, grants no F016, Z63, P15382), the DFG (Germany, grants no SPP1053, HE1049, KL1077) and the VW-Foundation (Germany, grant no I/79 227).

References

- [1] Einstein A 1905 *Ann. Phys., Lpz.* **17** 132
- [2] Lenard P 1902 *Ann. Phys., Lpz.* **8** 149

-
- [3] Bransden B H and Joachain C J 1983 *Physics of Atoms and Molecules* (London: Longman) p 55
 - [4] Diels J C and Rudolph W 1996 *Ultrashort Laser Pulse Phenomena: Fundamentals, Techniques, and Applications on a Femtosecond Time Scale* (New York: Academic)
 - [5] Attwood D 1999 *Soft X-Rays and Extreme Ultraviolet Radiation: Principles and Applications* (Cambridge: Cambridge University Press)
 - [6] Steinmeyer G D, Sutter H, Gallmann L, Matuschek N and Keller U 1999 *Science* **286** 1507
 - [7] Zewail A 2000 *J. Chem. Phys. A* **104** 5660
 - [8] Niikura H *et al* 2002 *Nature* **417** 917
 - [9] Sartania S *et al* 1997 *Opt. Lett.* **22** 1562
 - [10] Xu L, Spielmann Ch, Poppe A, Brabec T, Krausz F and Hänsch T W 1996 *Opt. Lett.* **21** 2008
 - [11] Jones D J 2000 *Science* **288** 635
 - [12] Apolonski A *et al* 2000 *Phys. Rev. Lett.* **85** 740
 - [13] Holzwarth R *et al* 2000 *Phys. Rev. Lett.* **85** 2264
 - [14] Hänsch T W 1997 private communication
 - [15] Telle H R *et al* 1999 *Appl. Phys. B* **69** 327
 - [16] Reichert J, Holzwarth R, Udem Th and Hänsch T W 1999 *Opt. Commun.* **172** 59
 - [17] Baltuska A *et al* 2003 *Nature* **421** 611
 - [18] Lewenstein M, Balcou P, Ivanov M Y, Huillier A L and Corkum P B 1994 *Phys. Rev. A* **49** 2117
 - [19] Corkum P B 1993 *Phys. Rev. Lett.* **71** 1994
 - [20] Schafer K J, DiMauro L F and Kulander K C 1993 *Phys. Rev. Lett.* **70** 1599
 - [21] Paul P M *et al* 2001 *Science* **292** 1689
 - [22] Tzallas P, Charalambidis D, Papadogiannis N A, Witte K and Tsakiris G D 2003 *Nature* **426** 267
 - [23] Drescher M, Hentschel M, Kienberger R, Tempea G, Spielmann C, Reider G, Corkum P and Krausz F 2001 *Science* **291** 1923
 - [24] Kienberger R *et al* 2004 *Nature* **427** 817
 - [25] Goulielmakis E *et al* 2004 *Science* **305** 1267
 - [26] Glover T E, Schoenlein R W, Chin A H and Shank C V 1996 *Phys. Rev. Lett.* **76** 2468
 - [27] Aksela H, Aksela S and Pulkkinen H 1984 *Phys. Rev. A* **30** 2456
 - [28] Schmidtke B, Khalil T, Drescher M, Müller N, Kabachnik N M and Heinzmann U 2001 *J. Phys. B: At. Mol. Opt. Phys.* **34** 4293
 - [29] Drescher M *et al* 2002 *Nature* **419** 803
 - [30] Jurvansuu M, Kivimäki A and Aksela S 2001 *Phys. Rev. A* **64** 012502
 - [31] Martensson N and Nyholm R 1981 *Phys. Rev. B* **24** 7121
 - [32] Smirnova O, Yakovlev V and Scrinzi A 2003 *Phys. Rev. Lett.* **91** 253001
 - [33] Seres J 2005 *Nature* **433** 596